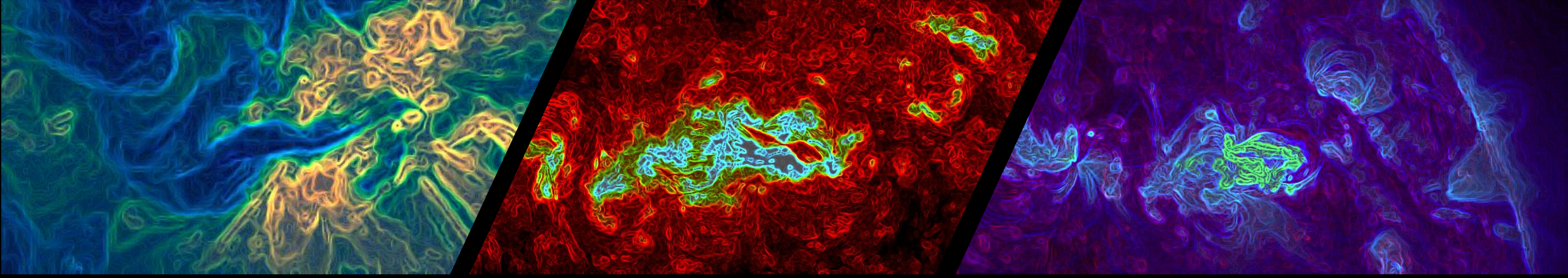

CME modelling with FRi3D in EUHFORIA using **EUI** data for input parameter estimation: twist and magnetic flux associated with a solar magnetic flux rope

Brenda D. Dorsch
Luciano Rodriguez
Jasmina Magdalenić

EUI-Metis workshop
Brussels, 2025.

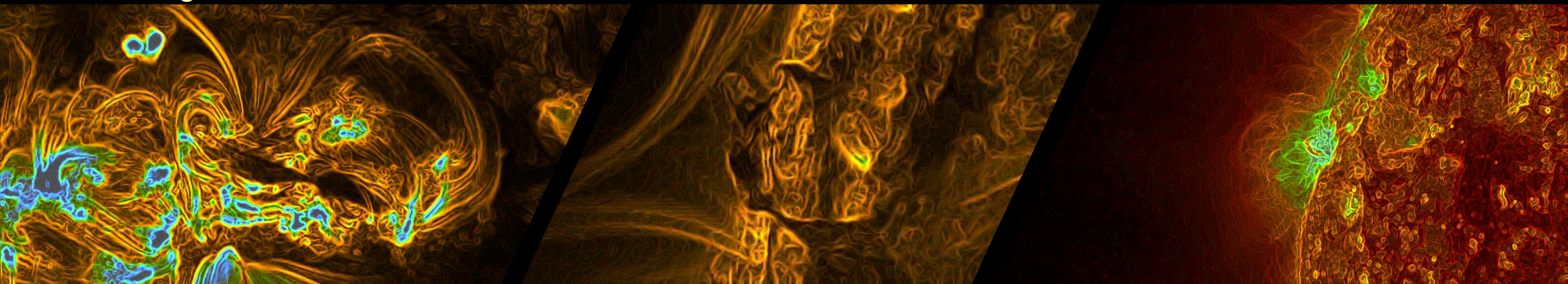

Introduction – *Coronal Mass Ejections (CMEs)*

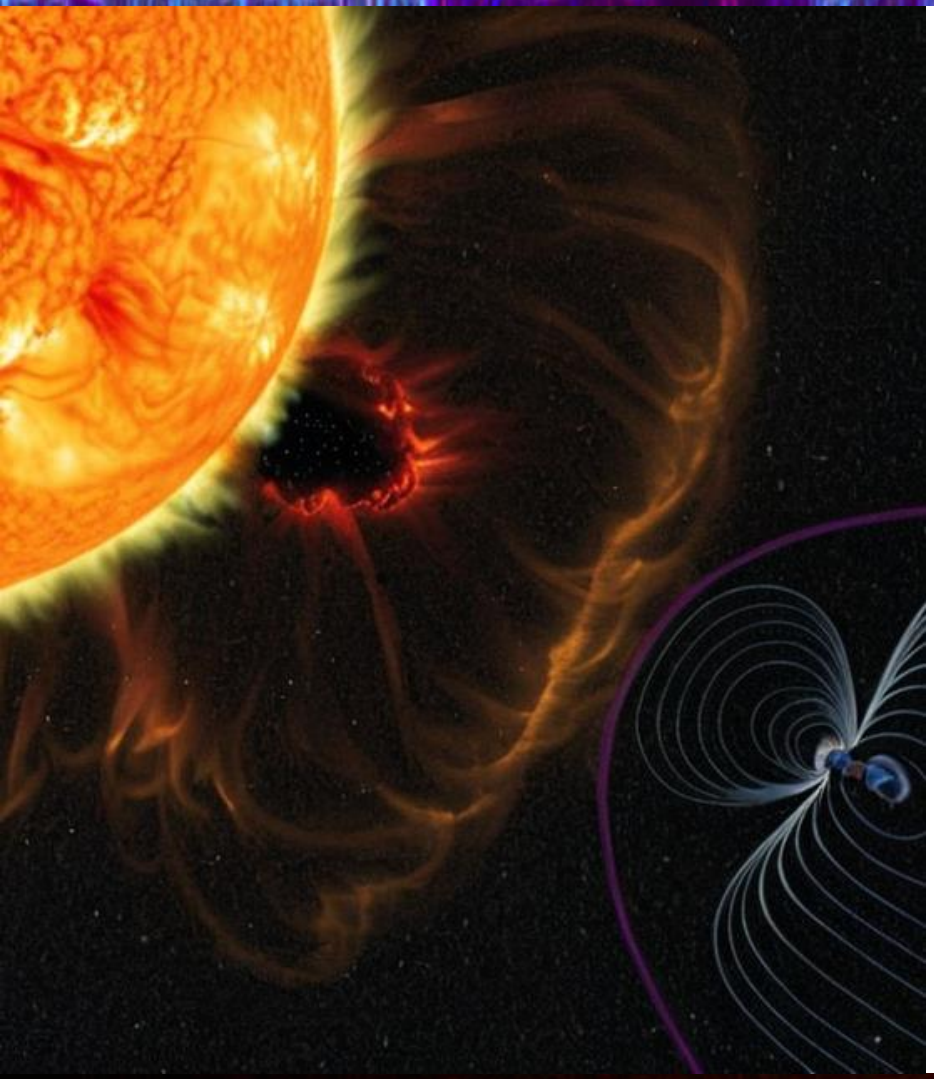

Eruptions of plasma and magnetic field from the Sun's corona.

Drivers of the most intense geomagnetic storms.

Key CME parameters for analysis: angular width, speed, direction, and magnetic field (inferred from ***spacecraft*** data).

Improving accuracy of space weather prediction.

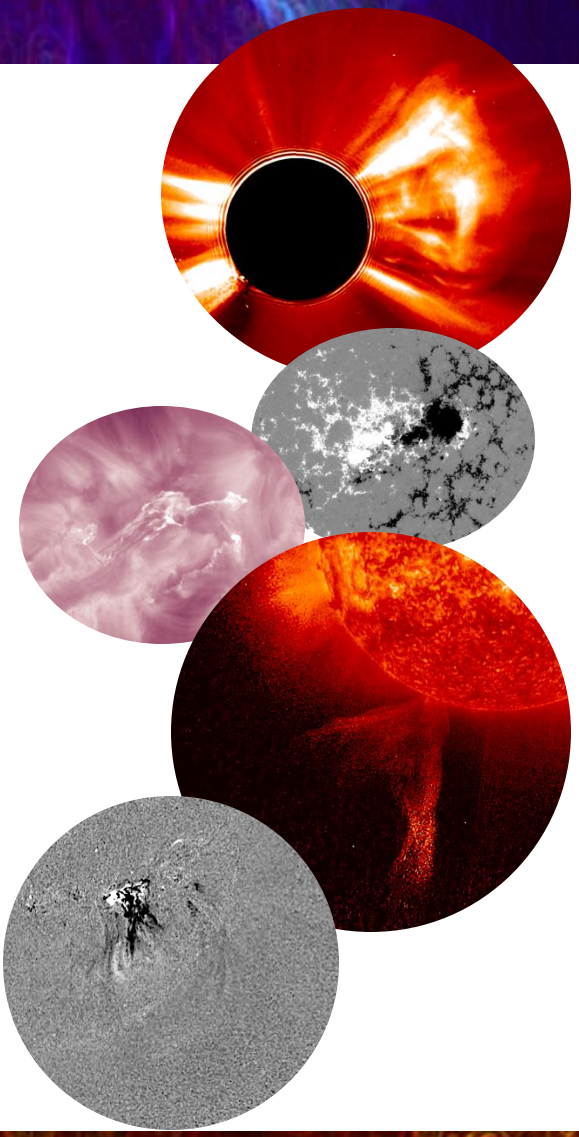

Introduction – *EUHFORIA*

European Heliospheric FORecasting Information Asset.

Pomoell & Poedts 2018.

Space weather forecasting-targeted inner heliosphere model.

Two major components

Coronal model:
Provides data-driven solar wind plasma parameters at 0.1 AU.

Heliospheric model:
Use boundary conditions to drive a 3D time-dependent MHD model of the inner heliosphere up to 2 AU.

CMEs are injected at the inner boundary of EUHFORIA.
Different **CME models** can be implemented.

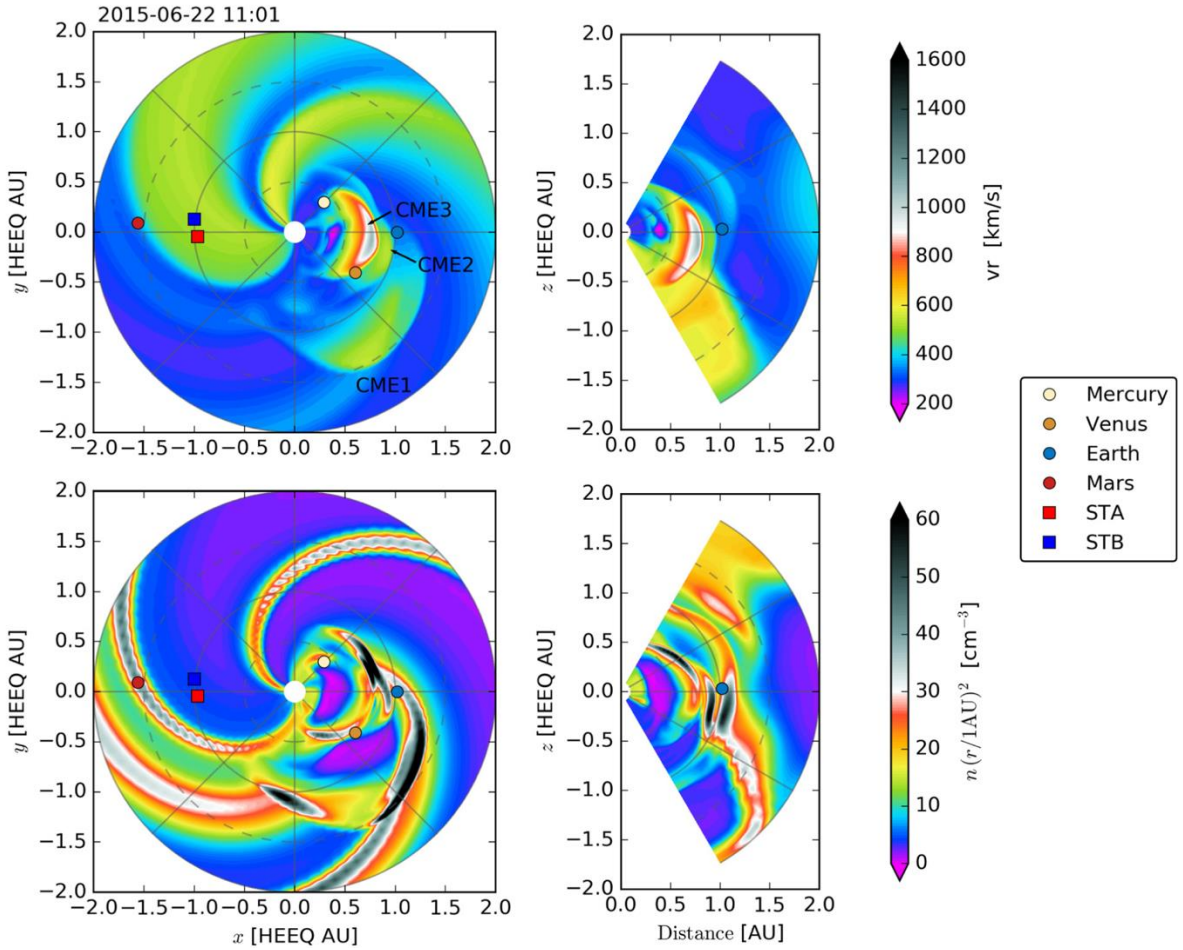

Introduction – FRi3D model

Flux rope with extended geometry.

17 CME input parameters:

- Plasma.
- Geometrical.
- Deformation.
- Magnetic field.

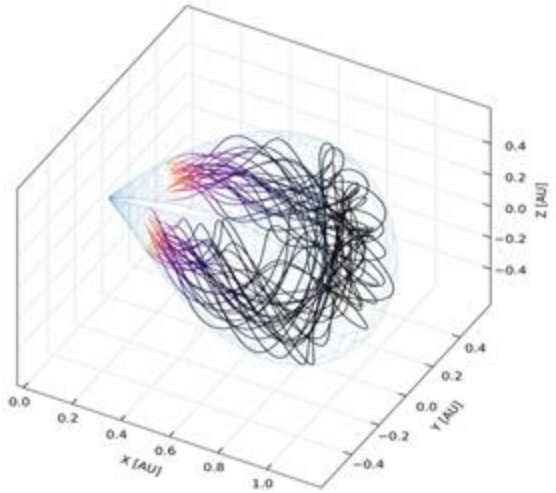

Total magnetic flux.

Twist.

Chirality.

Polarity.

Tilt.

Estimated from the EUV & magnetogram data.

Quantifies the rotation of the magnetic field lines around its axis.
Difficult to estimate; a **default** value is often used in CME modelling.

Handedness and direction of the axis of the flux rope.
⇨ Obtained directly from analysis of EUV images.

Angular orientation of the CME axis.
⇨ Retrieved form 3D reconstruction.

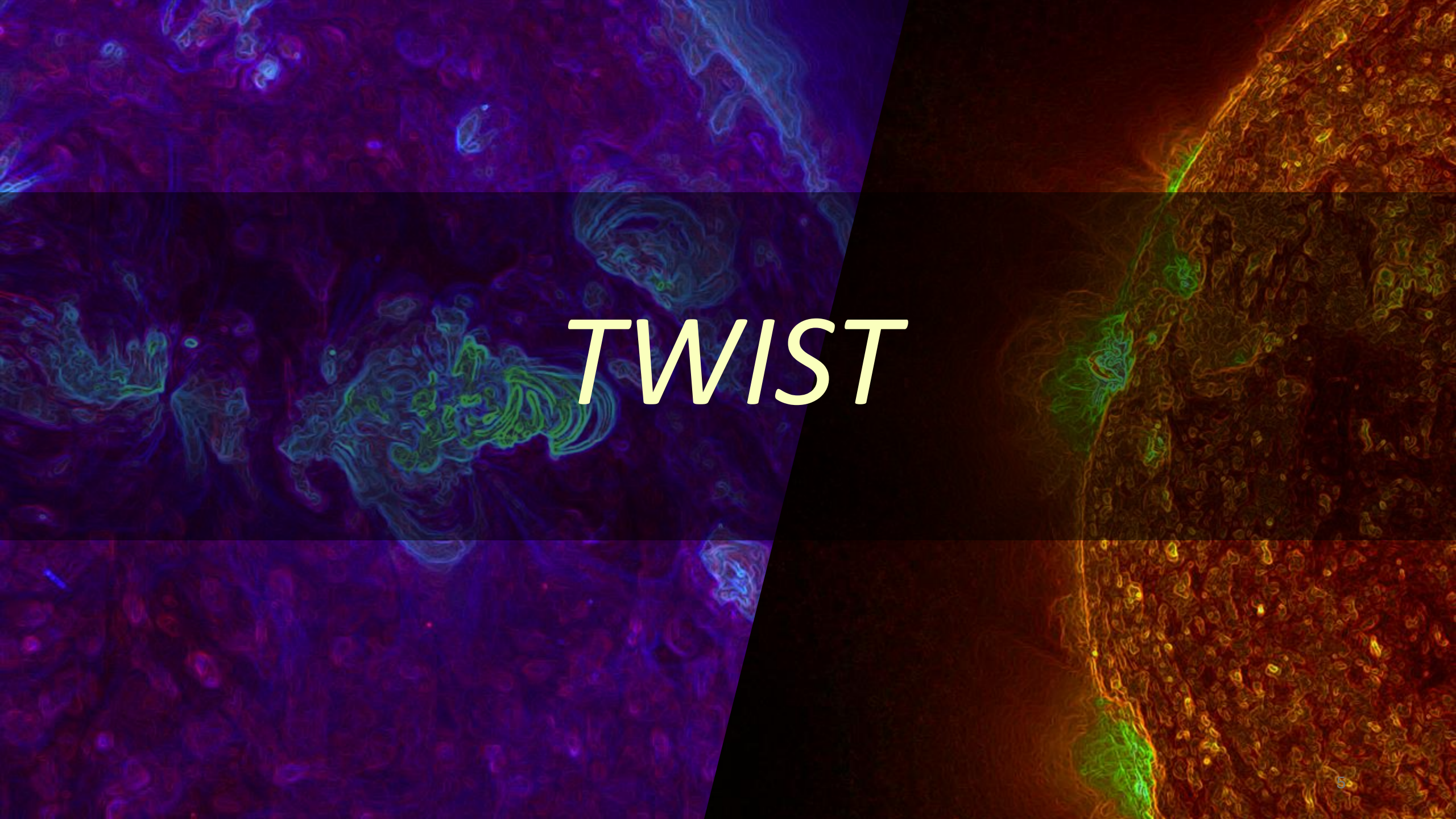
TWIST

Twist – *Motivation*

How accurate is to use a default twist value?

We performed number of runs with FRi3D for one CME event, **changing** the **twist** value in each run.

Results demonstrated the parameter's impact on simulation results.

Affects mainly
speed & **magnetic intensity**.

This highlights the **importance** of having a method to **constrain** the twist.

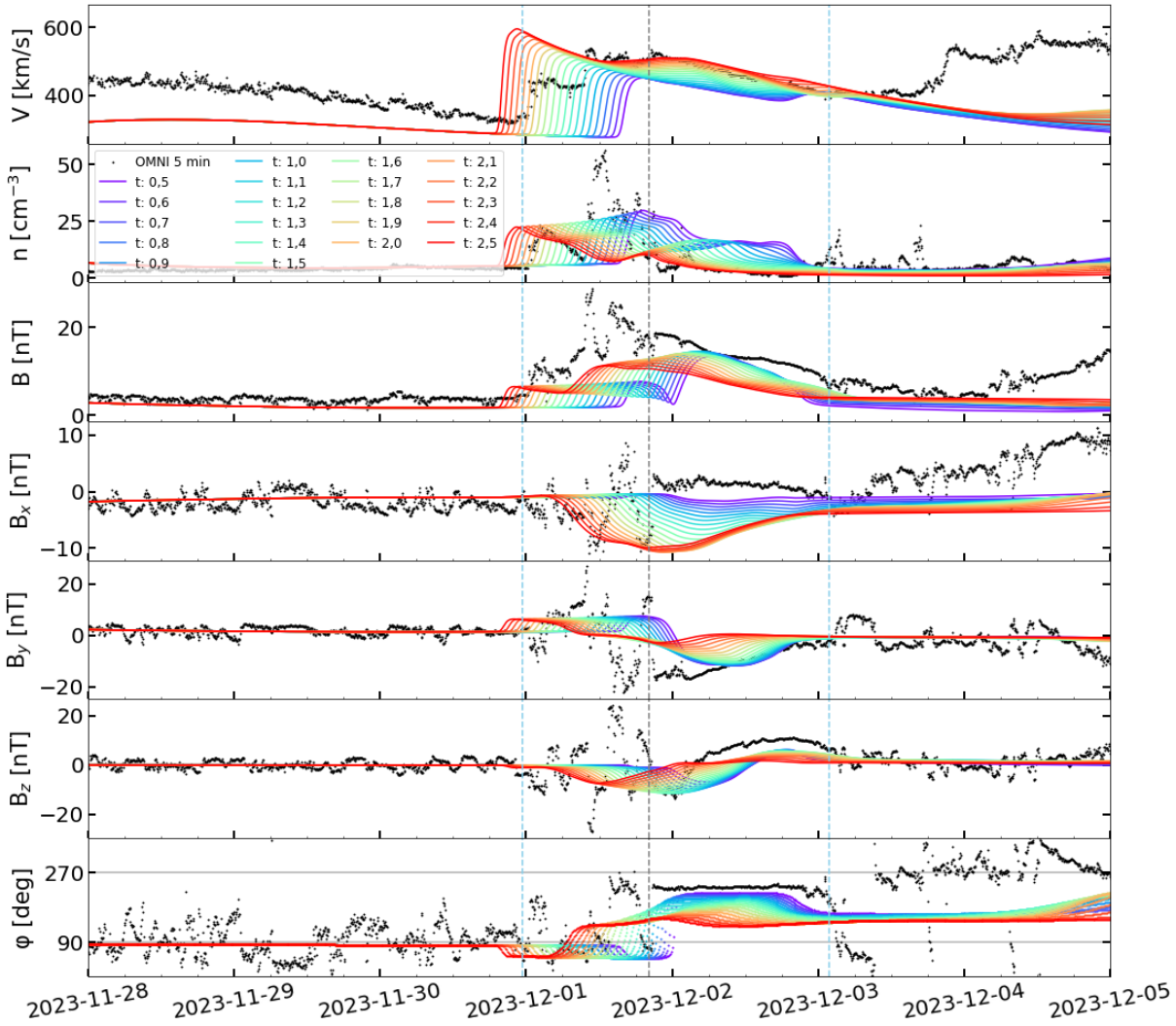

Twist – *Constraining methodology*

We aim for a methodology that:
- Is suitable also in operational forecasting.
- Employs data available in real-time.

$$|T_w| = 0.26\frac{L}{r} - 0.15$$

J. H. Guo, et al., 2021.

L & ***r*** Length & small radius of a flux rope.

3D reconstruction

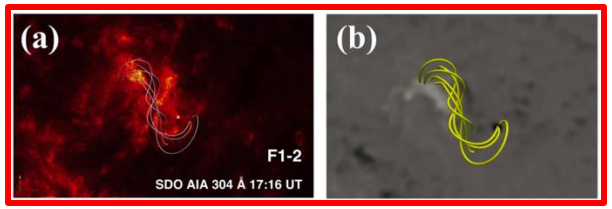

We propose to use a EUV image, i.e., **2D approach**, using the **width** instead of the small radius.

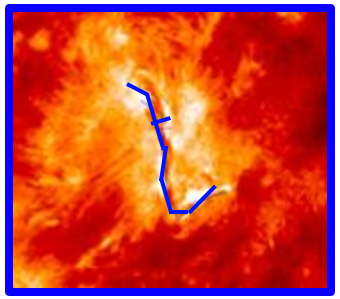

Limitations.

Projection effects.

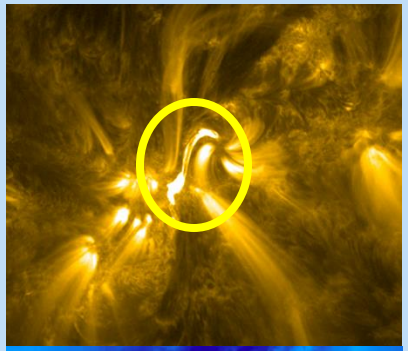

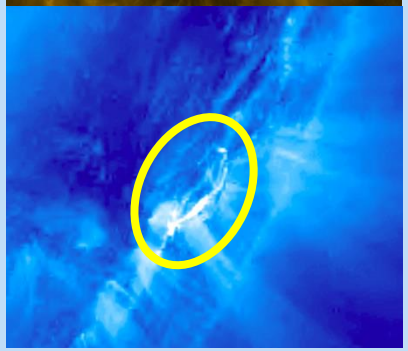

Complexity of the region.

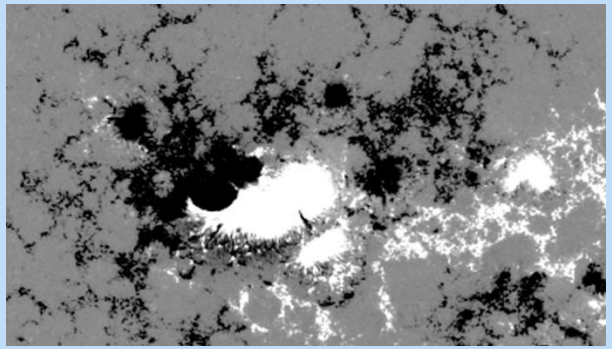

EUV wavelength.

Solar structures visible in the specific EUV image employed.

Twist – *tool development*

Interactive tool.

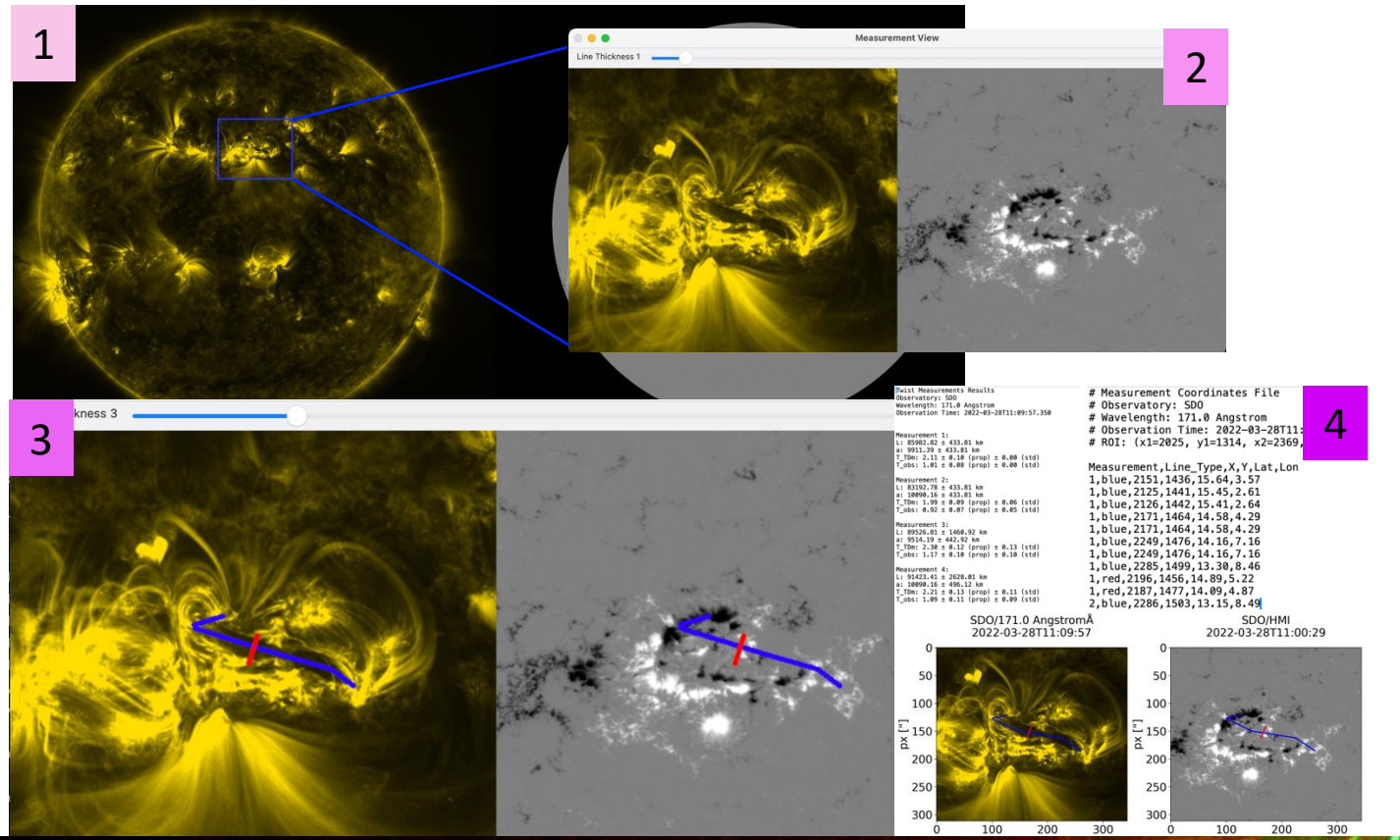

1- Region selection.

2- **Interactive** pop-up window with selected region. **EUV** image on the left. HMI **magnetogram** on the right, to help with identification of flux rope foot points.

3- Drawing of flux rope length (blue lines) & width (red line). **Measurements** can be repeated few times before closing the interactive window.

4- Saving measurements information.

Twist – *Study*

We measured characteristics of **34** solar flux ropes, were a CME was associated.

We used: **SolO**, **SDO** & **STEREO**.

5 measurements per *event & instrument*, we take the average value.

By using observations from **multiple spacecraft**, we address the **projection** effect.

CME kinematics form 3D reconstruction.

Use of coronagraph images.

No	Date [aaaa-mm-dd]	Time [UT]	Instrument	$\lvert \overline{T_W} \rvert$ (turns)	Lon[1] [°]	$\lvert \overline{T_{W_b}} \rvert^2$ (turns)	$\overline{L}$ [Km]	$\bar{a}$ [Km]	L/a	V_{CME} [Km/s]	Flare[3]	AR[4]
1	2012-07-12	16:10	AIA 171 Å	1.93 ± 0.11	0	1.93	141472	17749	8	1335	X	$\beta\gamma$
2	2014-09-10	17:18	AIA 171 Å	1.28 ± 0.06	5	1.28	112352	20521	5	1136	X	$\beta\gamma\delta$
3	2020-12-07	14:33	AIA 171 Å	2.77 ± 0.49	8	2.90	58327	5213	11	1179	C	α
		14:32	EUVI 171 Å	1.78 ± 0.62	70		51876	7000	7			
4	2021-10-28	15:24	AIA 171 Å	2.77 ± 0.24	0	2.77	119623	10744	11	1078	X	$\beta\gamma$
		15:23	EUVI 171 Å	2.39 ± 0.52	42		105766	10822	10			
5	2022-01-29	20:50	AIA 171 Å	2.15 ± 0.32	0	2.10	61437	6998	9	671	M	$\beta\gamma\delta$
		20:50	EUVI 171 Å	1.63 ± 0.22	28		55887	8288	7			
		20:52	EUI 174 Å	1.80 ± 0.40	12		61941	8703	7			
6	2022-02-06	12:04	AIA 171 Å	2.89 ± 0.43	2	2.90	255524	22302	11	650	C	β
		12:02	EUVI 195 Å	2.31 ± 0.37	36		239944	25646	9			
		12:02	EUI 174 Å	2.47 ± 0.41	21		264895	26600	10			
7	2022-03-28	11:09	AIA 171 Å	2.13 ± 0.13	5	2.13	87853	10020	9	636	M	$\beta\gamma$
		11:09	EUVI 171 Å	1.59 ± 0.31	40		71446	10775	7			
		11:10	EUI 174 Å	1.31 ± 0.37	80		71177	13075	5			
8	2022-03-28	18:48	AIA 171 Å	1.84 ± 0.14	9	1.95	57352	7493	8	836	M	$\beta\gamma$
		18:45	EUVI 195 Å	1.41 ± 0.22	44		53444	8901	6			
9	2023-10-16	10:30	AIA 171 Å	1.93 ± 0.18	49	2.63	103126	13192	8	787	C	α
		10:31	EUVI 17195 Å	1.63 ± 0.42	53		98573	14790	7			
		10:30	EUI 174 Å	2.50 ± 0.43	7		125142	12571	10			
10	2023-11-27	18:14	AIA 171 Å	3.07 ± 0.56	15	3.63	192583	15892	12	540	C	α
		18:15	EUVI 195 Å	2.90 ± 0.38	21		209885	18066	12			
		18:13	EUI 174 Å	3.46 ± 0.44	5		236521	17439	14			
11	2023-11-27	23:00	AIA 171 Å	3.78 ± 0.41	47	4.59	647844	43276	15	1000	-	-
		23:00	EUVI 195 Å	3.37 ± 0.18	55		622676	43245	14			
		23:00	EUI 174 Å	3.86 ± 0.39	33		683017	44828	15			
12	2023-11-28	19:13	AIA 171 Å	1.98 ± 0.57	0	1.98	118057	14815	8	791	M	$\beta\gamma$
		19:13	EUVI 171 Å	1.8 ± 0.3	5		121735	16621	7			
		19:13	EUI 174 Å	1.54 ± 0.41	12		115459	18833	6			
13	2024-01-02	18:11	AIA 171 Å	1.86 ± 0.35	52	2.79	81371	10712	8	510	M	$\beta\gamma$
		18:12	EUVI 195 Å	1.58 ± 0.18	60		79778	12063	7			
		18:11	EUI 174 Å	2.07 ± 0.2	36		87444	10442	8			
14	2024-01-09	20:09	AIA 171 Å	1.69 ± 0.17	72	2.66	102193	14574	7	717	-	-
		20:09	EUVI 171 Å	1.38 ± 0.15	82		127898	21913	6			
		20:11	EUI 174 Å	1.84 ± 0.4	53		118091	15601	8			

								$\bar{a}$ [Km]	L/a	V_{CME} [Km/s]	Flare[3]	AR[4]
							.7	43985	12	957	-	-
							0	51601	11			
							2	44538	10			
							8	12884	7	744	C	α
							2	15023	7			
							4	14960	6			
							3	13171	10	544	C	β
							4	12545	9			
							8	14222	9			
							7	17219	10	1168	X	$\beta\gamma\delta$
							1	17587	9			
							3	16411	9			
							8	23991	10	-	C	$\beta\gamma$
							1	24101	11			
		09:01	EUI 174 Å	2.15 ± 0.26	29			235393	26827	9			
20	2025-01-21	09:39	AIA 171 Å	2.43 ± 0.24	25	2.85		206537	20953	10	760	M	$\beta\gamma$
		09:38	EUVI 171 Å	2.22 ± 0.72	53			159198	17971	9		
		09:36	EUI 174 Å	2.83 ± 0.44	6			259151	22708	11		
21	2025-01-22	10:37	AIA 171 Å	2.33 ± 0.25	11	2.68		135363	14356	9	572	M	$\beta\gamma$
		10:38	EUVI 171 Å	1.99 ± 0.30	17			138659	17154	8		
		10:37	EUI 174 Å	1.61 ± 0.55	30			138436	20812	7		

[1] Absolute longitude relative to the spacecraft.
[2] Average twist value de-projected to the central meridian.
[3] Flare class.
[4] Hale classification.

Twist – *Study*

Examples.

SDO/AIA

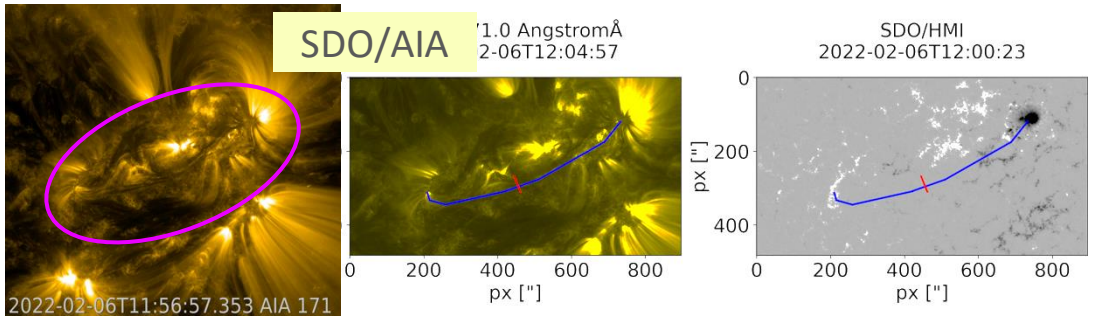

STEREO/SECCHI

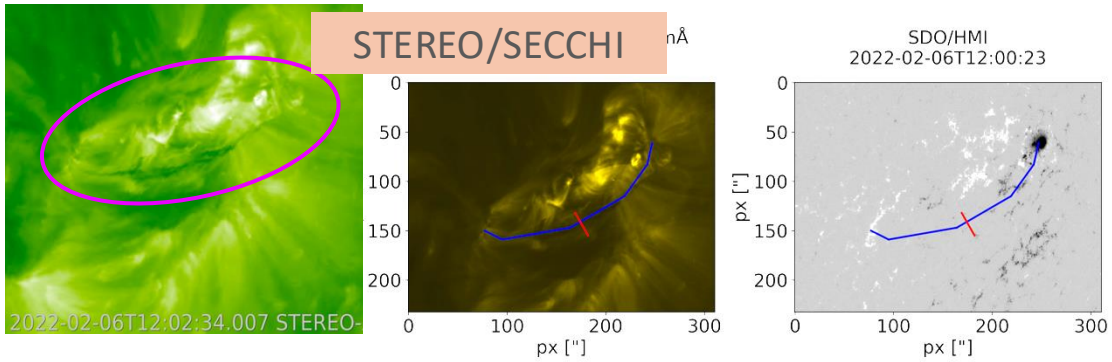

SolO/EUI

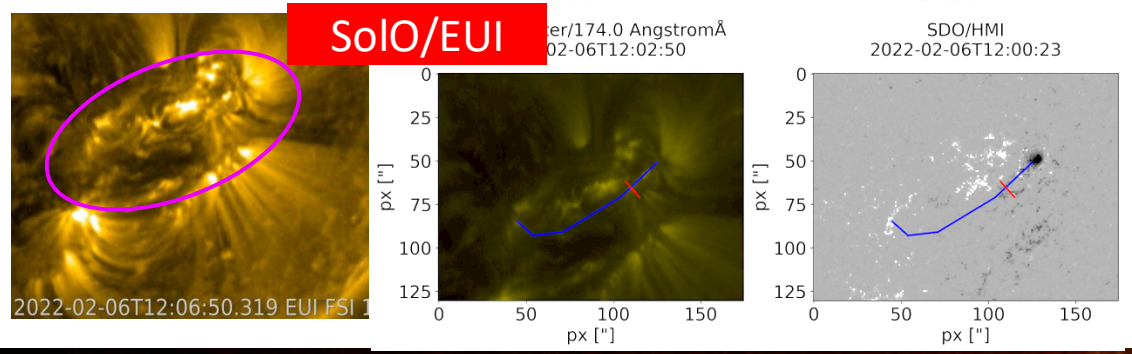

SDO/AIA

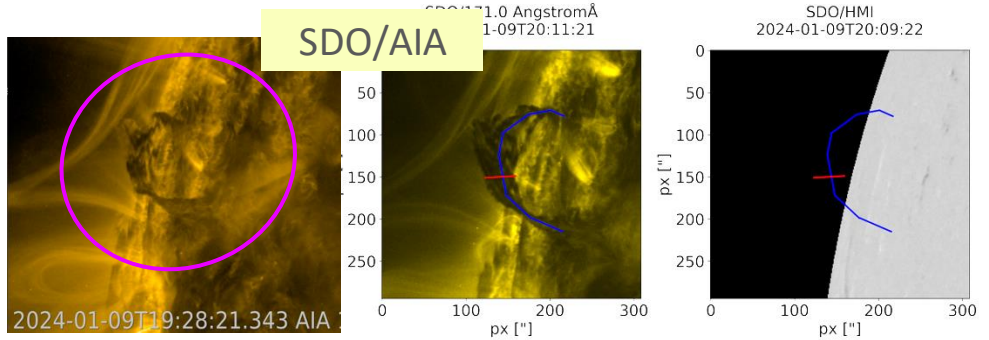

STEREO/SECCHI

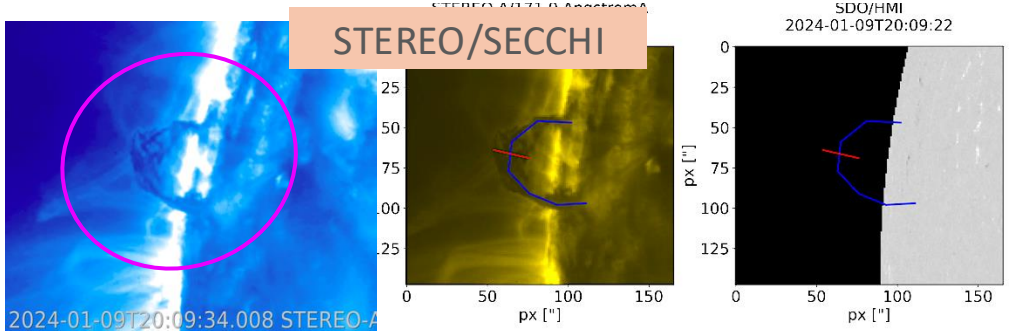

SolO/EUI

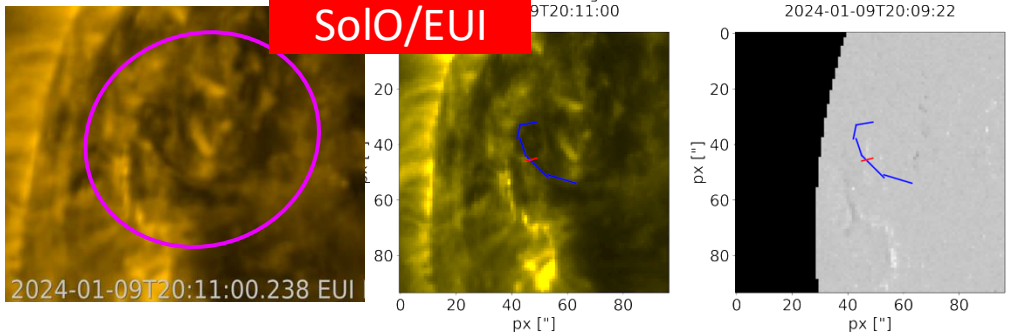

Twist – *Study*

Coherent dependence of twist with relative longitude of the event.

The twist value decreses closer to the limb.

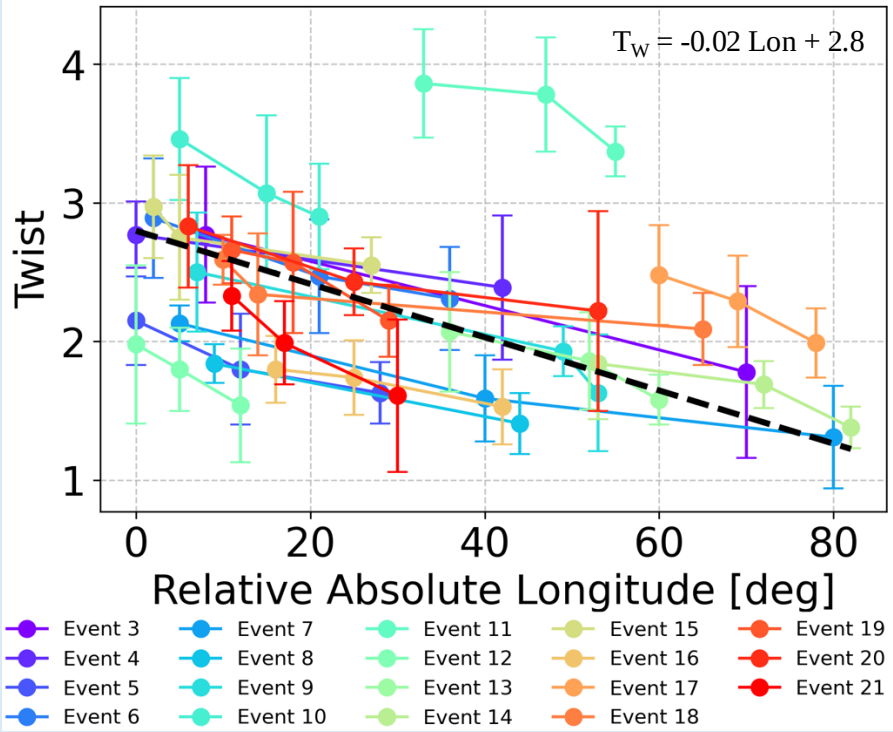

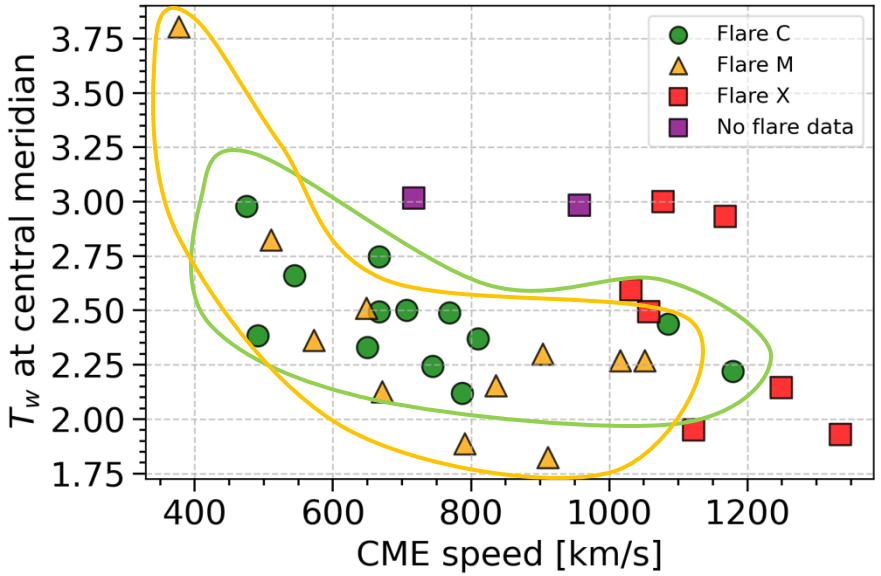

Subgroups showing different behaviour?

Data suggest a relationship between T_W and CME speed, in particular for events associated to C-class and M-class flares subgroups.

No conclusive relation for events associated to X-class flares.

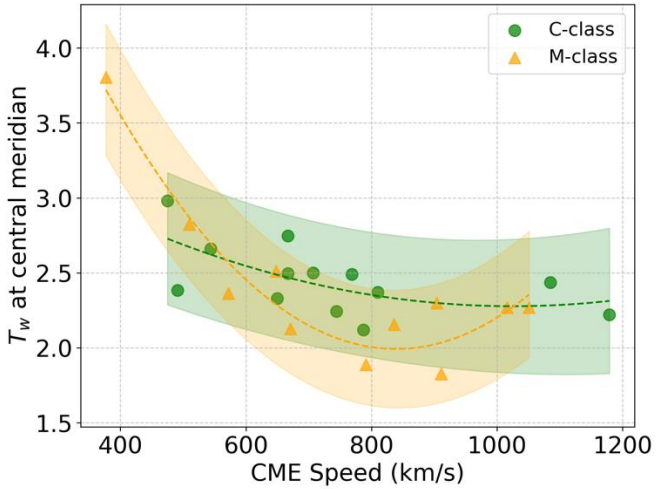

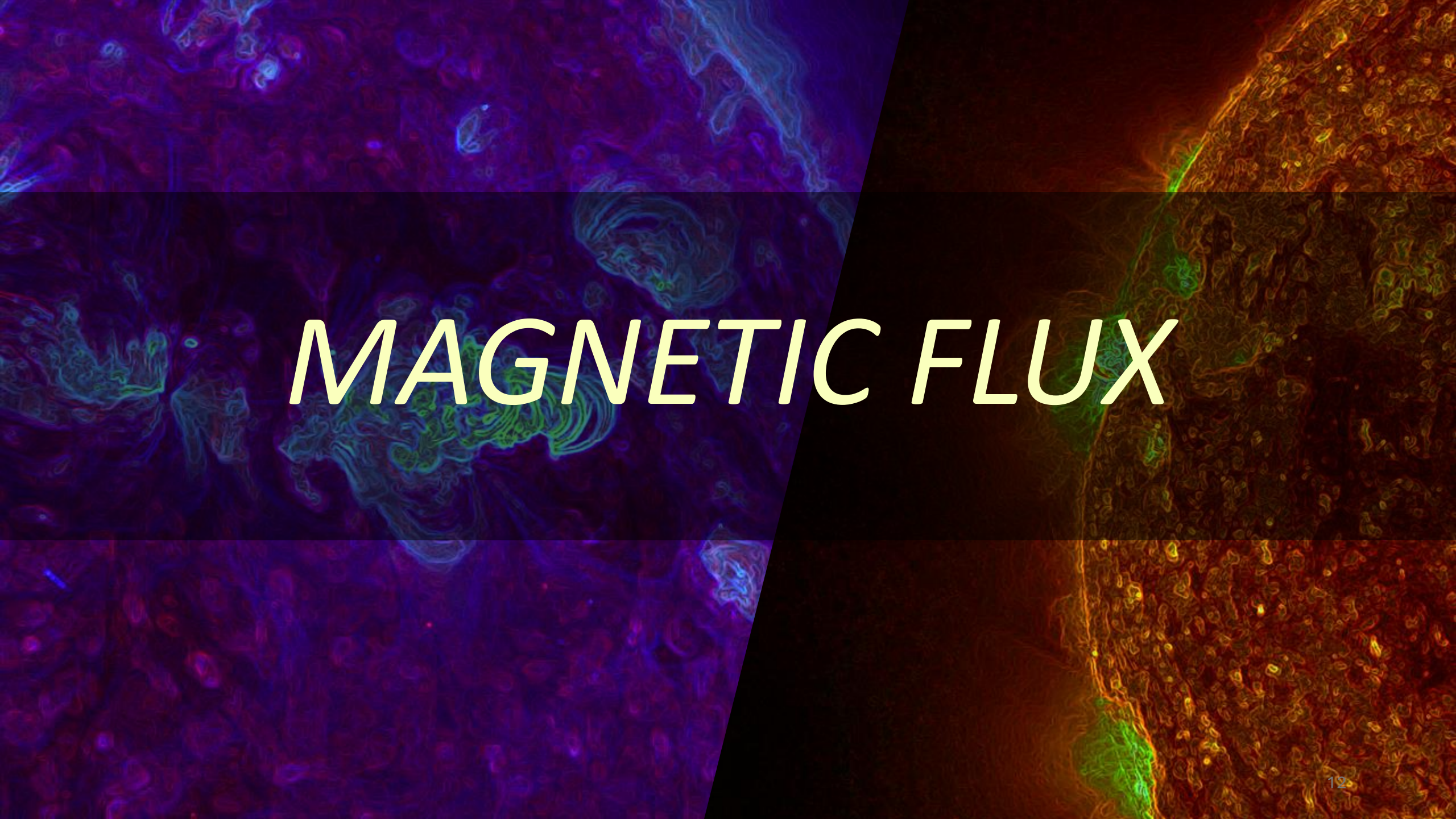
MAGNETIC FLUX

Magnetic flux – *Constraining methodology*

Reconnection flux can be equated to the **poloidal flux** of the flux rope.

Estimation:

→ Ribbon method.

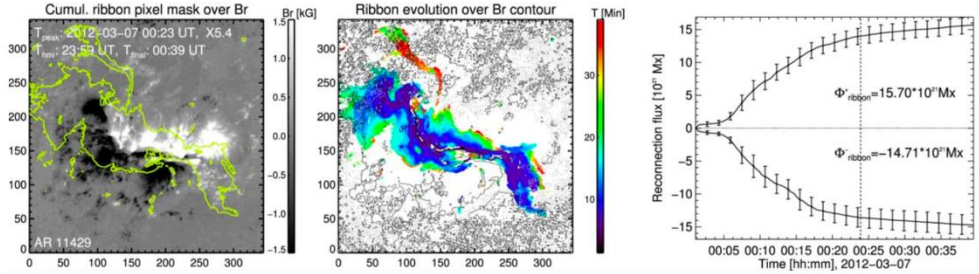

→ PEA (Post-Eruption Arcades) method.

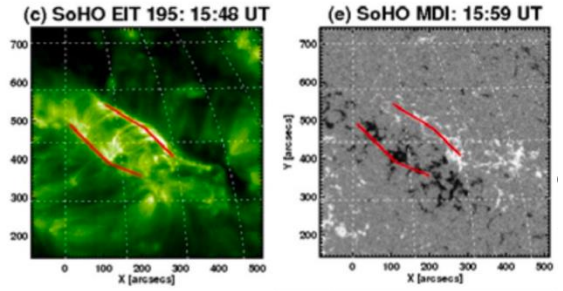

Gopalswamy et al., 2017.

Poloidal or azimuthal magnetic flux

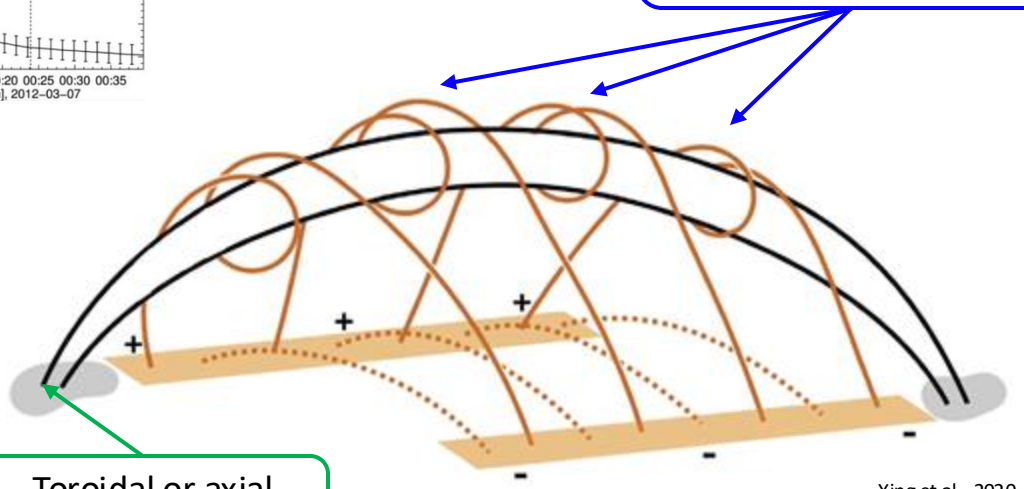

Toroidal or axial magnetic flux

Xing et al., 2020.

Magnetic flux – Constraining methodology

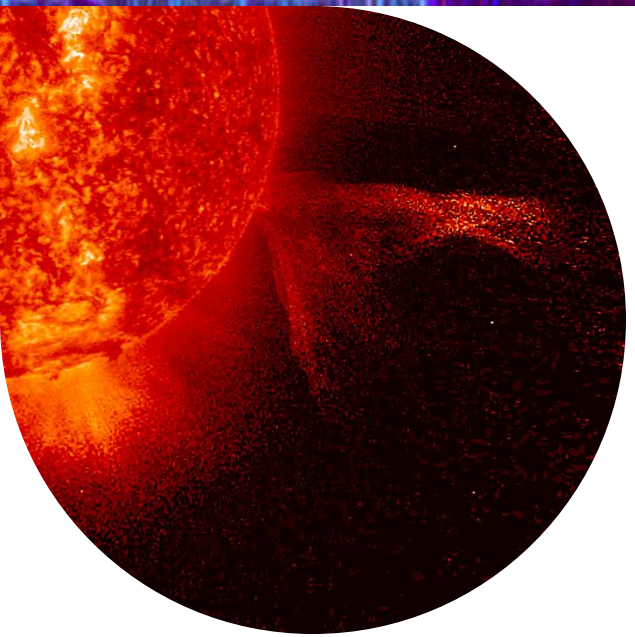

Contrary to Ribbon method, **PEA method** does not need data with high cadence. ⟷ **1** EUV file. **1** magnetogram file.

Better for the forecasting workflow.

SolO data can be used →
EUI + PHI

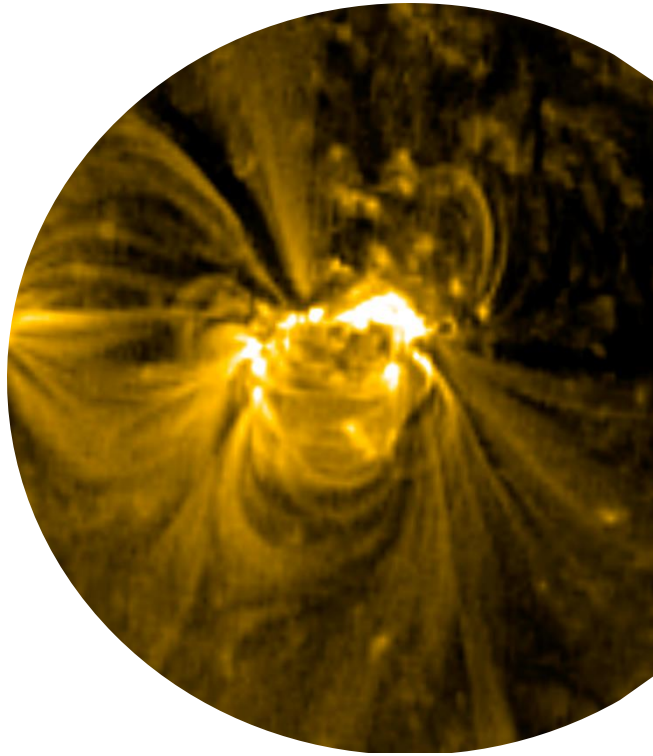

Magnetic flux – tool development

Interactive tool.

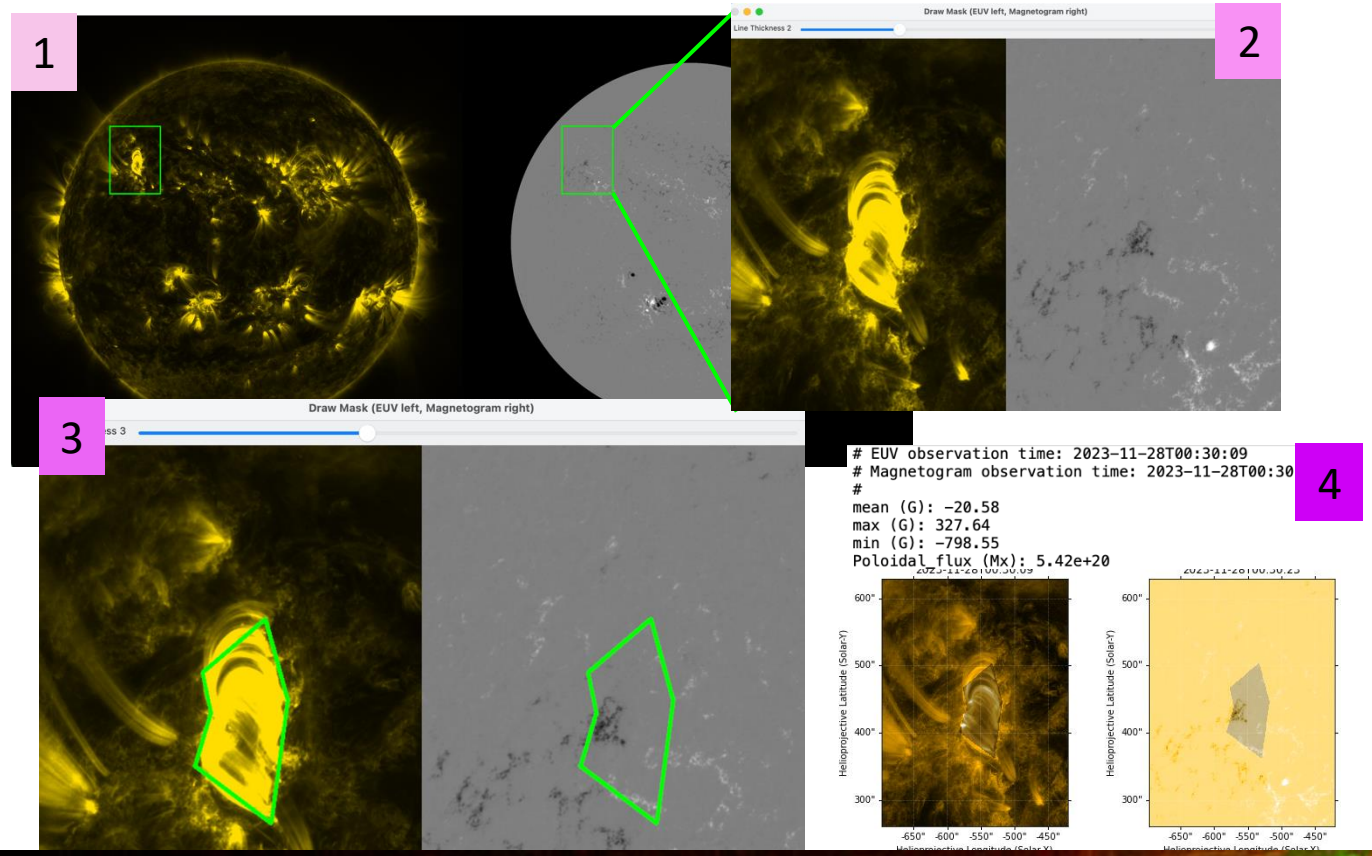

1- Region selection.

2- Interactive pop-up window with selected region. **EUV** image on the left. **Magnetogram** on the right.

3- Drawing the PEA region to create a mask that will be used to **calculate** the poloidal magnetic flux **from the magnetogram**.

4- Saving measurements information.

Magnetic flux – Implementation

Developed python code to calculate poloidal flux with SDO.

Adapt the code to use it with SolO.

Validation.

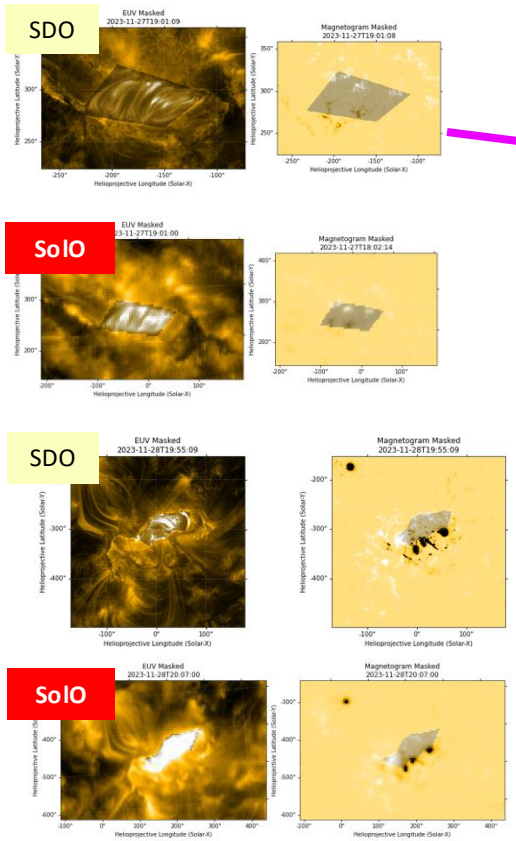

Date	Spacecraft	Poloidal magnetic flux [Mx]
2023-11-27	SDO	$0.490e^{21}$
	SolO	$0.496e^{21}$
2023-11-28	SDO	$0.542e^{21}$
	SolO	$0.562e^{21}$
2023-11-28	SDO	$1.62e^{21}$
	SolO	$1.49e^{21}$
2023-12-02	SDO	$1.65e^{21}$
	Solo	$1.14e^{21}$

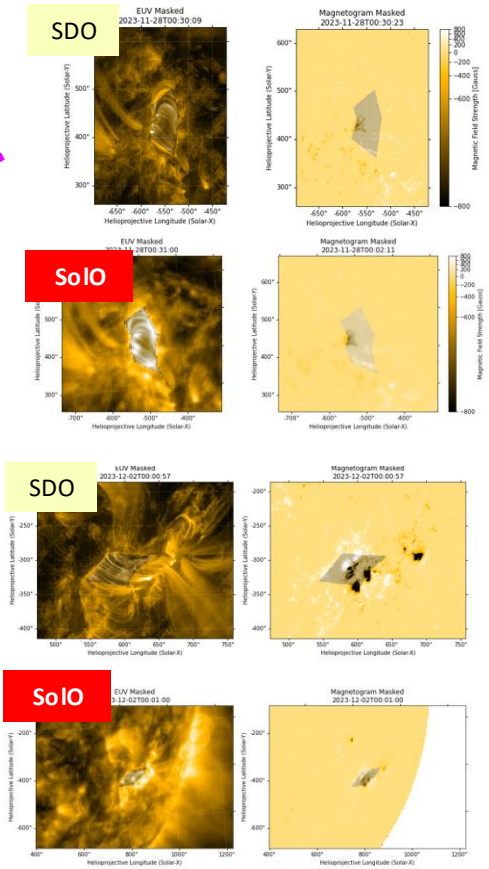

Events where spacecraft have a **similar FOV**.

Separation angle between **SDO & SolO** ~ 11 deg.

Summary & Conclusions

- Is important to **constrain** the twist parameter and not relying on a default value for CME modelling.
- We adapted a formula that estimates twist from the ratio ***L/a*** for use with a ratio derived from an **EUV image &** we **developed a tool** to apply the methodology.

- We **developed a tool** to estimate **magnetic flux** from the PEA method for magnetized CME models, using **EUI & PHI data**.

- We studied the ***twist*** for **34 flux rope** events, observed with SDO, **SolO (EUI)** & STEREO.
- **Projection effect**: Twist measurements show a consistent dependence on the structure's projection, regardless of the spatial resolution of the instruments used.
- Data suggests a relationship between $\mathbf{T_W}$ and **CME speed**, in particular for **C-class** and **M-class** flare subgroups.

THANK YOU!!